ROYAL SOCIETY OPEN SCIENCE

royalsocietypublishing.org/journal/rsos

Research

Cite this article: Martin KR, Mansfield KL, Savage AE. 2022 Adaptive evolution of major histocompatibility complex class I immune genes and disease associations in coastal juvenile sea turtles. *R. Soc. Open Sci.* **9**: 211190. https://doi.org/10.1098/rsos.211190

Received: 15 July 2021
Accepted: 6 January 2022

Subject Category:
Genetics and genomics

Subject Areas:
evolution/genetics

Keywords:
immunogenetics, emerging infectious diseases, testudines, supertype, major histocompatibility complex, fibropapillomatosis

Author for correspondence:
Anna E. Savage
e-mail: anna.savage@ucf.edu

Electronic supplementary material is available online at https://doi.org/10.6084/m9.figshare.c.5823514.

THE ROYAL SOCIETY PUBLISHING

Adaptive evolution of major histocompatibility complex class I immune genes and disease associations in coastal juvenile sea turtles

Katherine R. Martin, Katherine L. Mansfield and Anna E. Savage

Department of Biology, University of Central Florida, 4110 Libra Drive, Orlando, FL 32816, USA

KRM, 0000-0002-1634-3484; KLM, 0000-0002-6568-2861; AES, 0000-0002-4917-8358

Characterizing polymorphism at the major histocompatibility complex (MHC) genes is key to understanding the vertebrate immune response to disease. Despite being globally afflicted by the infectious tumour disease fibropapillomatosis (FP), immunogenetic variation in sea turtles is minimally explored. We sequenced the α_1 peptide-binding region of MHC class I genes (162 bp) from 268 juvenile green (*Chelonia mydas*) and 88 loggerhead (*Caretta caretta*) sea turtles in Florida, USA. We recovered extensive variation (116 alleles) and trans-species polymorphism. Supertyping analysis uncovered three functional MHC supertypes corresponding to the three well-supported clades in the phylogeny. We found significant evidence of positive selection at seven amino acid sites in the class I exon. Random forest modelling and risk ratio analysis of *Ch. mydas* alleles uncovered one allele weakly associated with smooth FP tumour texture, which may be associated with disease outcome. Our study represents the first characterization of MHC class I diversity in *Ch. mydas* and the largest sample of sea turtles used to date in any study of adaptive genetic variation, revealing tremendous genetic variation and high adaptive potential to viral pathogen threats. The novel associations we identified between MHC diversity and FP outcomes in sea turtles further highlight the importance of evaluating genetic predictors of disease, including MHC and other functional markers.

1. Introduction

Infectious diseases threaten the conservation of biodiversity, particularly in species already at risk due to human-mediated

environmental change [1,2]. Environmental change such as warming temperatures and habitat fragmentation alters interactions between hosts and pathogens [3], often increasing pathogen load [4], altering host immune function [5] and leading to altered disease risk [6]. Emerging disease in ectothermic vertebrates is especially concerning in light of their sensitivity to global change [7]. In particular, variance in environmental thermal optima is linked to altered immune function in herpetofauna [8,9], and amphibians and reptiles are host to numerous emerging infectious diseases [10,11]. How well reptiles and amphibians can respond to novel disease regimes remains an important area of investigation for conservation biology. Species may adapt to pathogen pressure through immunogenetic evolution, particularly in major histocompatibility complex (MHC) genes [12]. Thus, the extent to which immunogenetic variation modulates disease outcomes in reptiles is a critical component for understanding their ability to persist, and remains an important and open question in wildlife conservation biology.

The MHC is a genomic region in jawed vertebrates encoding proteins that recognize and present foreign peptides to T-cells to initiate acquired immune responses [13]. Classical class I and II MHC genes encode glycoproteins with highly variable peptide-binding regions (PBRs) containing peptide-binding residues that bind antigens, thus determining whether targeted pathogen removal can be achieved [14]. The MHC class I PBR derives from α_1 and α_2 subunits encoded by exon 2 and exon 3, respectively [15]. MHC class I proteins are typically expressed endogenously and present viral pathogen particles, while class II proteins are only expressed on antigen-presenting cells and primarily recognize extracellular pathogens [14]. The diversity of expressed MHC proteins may indicate the host's ability to respond to a suite of different pathogens, with higher MHC variation typically associated with increased pathogen resistance [12,16]. MHC diversity is linked to pathogen immunity in numerous vertebrates [17–20] and is an important indicator of overall population health.

Sea turtles are long-lived, migratory and ancient reptiles that are globally afflicted by fibropapillomatosis (FP), an infectious disease that presents as internal and external neoplastic tumours [21]. FP is associated with chelonid alphaherpesvirus 5 (ChHV5) infection [22], but causal relationships with FP development remain unclear [23]. FP most commonly affects green sea turtles, *Chelonia mydas*, but is documented in all species of sea turtles [21,24–29] and predominantly affects immature turtles in coastal habitats [21] who have recruited to neritic waters after spending their first developmental years in the open ocean [30]. Juvenile *Ch. mydas* in the southeastern United States demonstrate high FP prevalence [31], including those found on the Florida Atlantic coast [32–34]. FP consequences range from complete tumour regression and recovery to turtle mortality [35,36]. Immunosuppression is associated with FP [37] and may develop after FP onset [26,38,39]. While the prevalence of FP in coastal habitats has led to speculation that environmental cofactors such as chemical pollutants and degraded environmental quality contribute to disease development [40,41], their precise role in FP aetiology remains uncertain. The interplay of FP, environmental change, pathogens and host immune defences has remained largely uncharacterized until recently, with studies indicating reduced or altered immune function in turtles with FP [39] and in turtles in degraded habitat [42], as well as differential immune expression in FP-afflicted *Ch. mydas* [43–46]. Given the importance of MHC in the acquired immune response, characterizing MHC diversity in coastal juvenile sea turtles may be particularly informative for understanding FP susceptibility.

To date, MHC studies in reptiles have mainly characterized gene diversity and evolutionary history, finding evidence of shared alleles between closely related species, high levels of polymorphism and evidence of positive selection in antigen-binding sites [47–49]. Even within reptiles, few immunogenetic studies examine turtles [50,51], and only one study has investigated MHC in sea turtles, describing two allele lineages recovered in a single loggerhead sea turtle (*Caretta caretta*) nesting population [52]. Here, we advance knowledge of MHC genetic variation and adaptive evolution in sea turtles by sampling juvenile *Ca. caretta* from a foraging aggregate and characterizing MHC in *Ch. mydas* for the first time. Quantifying MHC repertoires from both *Ca. caretta* and *Ch. mydas* lends insight into how MHC has evolved in sea turtles and more broadly facilitates our understanding of reptilian acquired immune systems. While a relationship between pathogen susceptibility and MHC genetic variation has been documented in tortoises [53,54], associations between MHC and disease in sea turtles remain unexplored. By sampling immature *Ch. mydas*, which are more commonly affected by FP than other species or age classes [31], we are thus able to explore potential associations between MHC and FP for the first time. The University of Central Florida Marine Turtle Research Group (MTRG) has sampled juvenile *Ch. mydas* and *Ca. caretta* for over 30 years at three sites on the Atlantic coast of Florida: the Indian River Lagoon (IRL), Trident Basin (TB) and Indian River County sabellariid worm rock reef (figure 1). Mean *Ch. mydas* FP prevalence is 48.9% in the IRL [33,34], 4.8% in TB [33] and 19% in the reef [33]. *Caretta caretta* FP prevalence is 4.5%

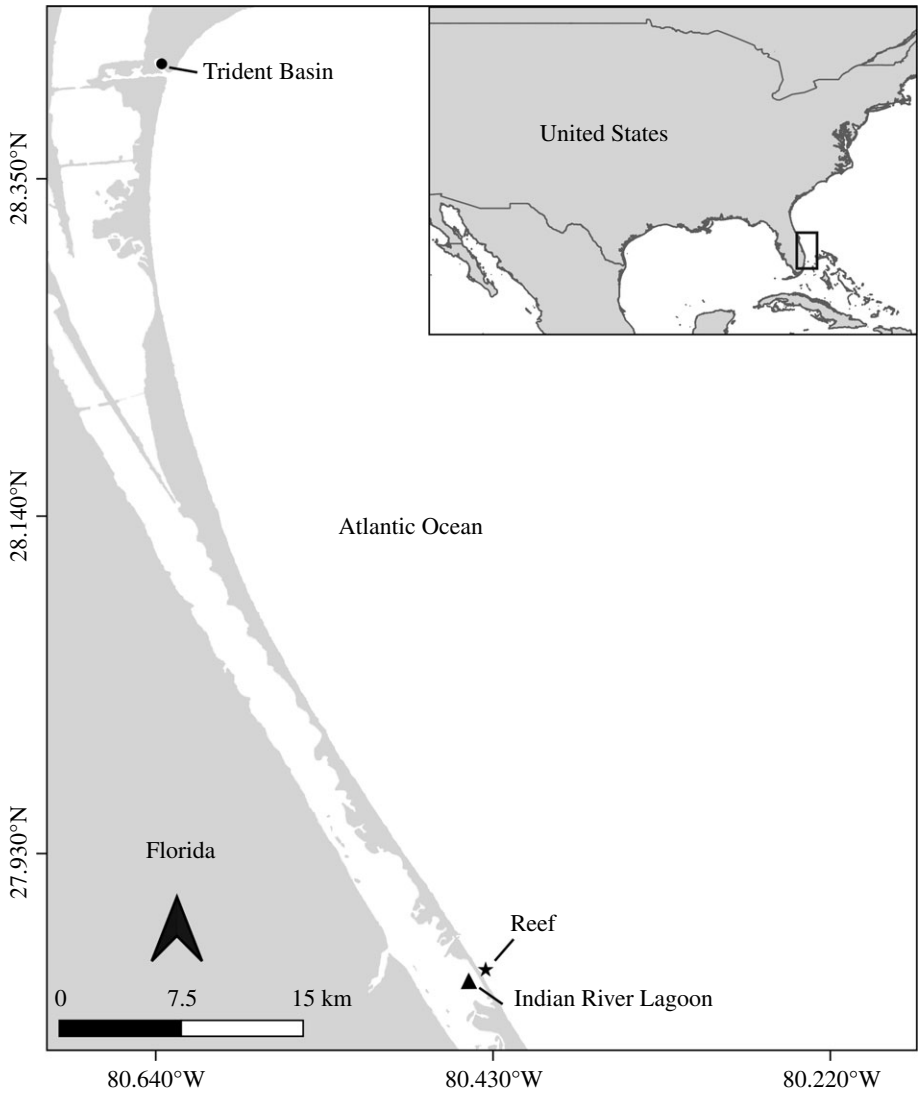

Figure 1. Study sites in central Florida where *Ch. mydas* and *Ca. caretta* juveniles are captured and sampled by the University of Central Florida Marine Turtle Research Group. TB is a military port adjacent to Port Canaveral, Florida; the IRL sampling site is located approximately 1–2 miles south of the Sebastian Inlet, Florida. Reef sampling occurred just offshore along the coastal beaches adjacent to the Sebastian Inlet, Florida.

in the IRL [55] and is unknown at the other sites due to low *Ca. caretta* encounter rates at those locations. Here, we leverage these long-term studies to characterize MHC class Iα diversity, molecular evolution and FP associations in Florida *Ch. mydas* and *Ca. caretta* juveniles to understand immunogenetic variation within and across species, and whether it predicts FP susceptibility. We identify novel MHC alleles from *Ch. mydas* and *Ca. caretta* and reconstruct a phylogeny to characterize MHC evolution and diversification. To examine how immunogenetics may affect FP dynamics, we model FP occurrence and smooth tumour texture (which may be associated with disease outcome [34]) in *Ch. mydas* as a function of our MHC and ecological dataset. Our study is the first MHC class Iα characterization in *Ch. mydas* and the first in any juvenile sea turtle, providing a robust foundation to understand immunogenetic shifts in sea turtles as they adapt to disease and other ecological changes.

2. Methods

2.1. Field methods

The MTRG has sampled the IRL twice a month since 1982 [55], TB twice a year since 1993 [56], and the reef (oceanside, approximately 5 km straight-line from the IRL), opportunistically from 1989 to 2010. We

used blood and skin collected from juvenile *Ch. mydas* and *Ca. caretta* across these sites between 1995 and 2018. Approximately 2 to 5 ml of blood were collected from the dorsal cervical sinus into heparinized blood collection tubes using the antiseptic protocol. Either 20 or 22 gauge, 1 inch needles were used, depending on the size of the turtle. The skin area to be biopsied was first scrubbed with an isopropyl alcohol swab and then a 4 mm sterile biopsy punch was used to sample a portion of the fleshy distal region of the rear flippers. A coagulant powder was used to control bleeding after sampling if needed. Tissues were preserved in 70% ethanol or heparinized tubes, and stored at −20°C for subsequent genetic analysis. The standardized straight carapace length (SCL) of each animal was measured using calipers. External tumours consistent with FP were photographed and scored according to severity [57]. We categorized tumour texture as either rough or smooth based on appearance and used these two categories in subsequent random forest (RF) and relative risk analyses to explore associations between tumour texture and MHC variation. Additionally, individuals that exhibited FP on initial capture that were subsequently recaptured with no external tumours were categorized as regressed ($n = 7$).

2.2. Major histocompatibility complex sequencing and bioinformatics

We extracted DNA from blood and skin samples using DNeasy extraction kits (Qiagen, Valencia, CA) and using conventional polymerase chain reaction (PCR), amplified 162 base pair (bp) of exon 2 of classical MHC class Iα genes (hereafter, MHC), which encode the α_1 subunit and the largest portion of the PBR. We used primers Cc-MHC-I-F (5′-GATGTATGGGTGTGATCTCCGGG-′3) and Cc-MHC-I-R (5′-TTCACTCGATGCAGGTCDNCTCCAGGT-′3) [52]. We performed amplifications in 20 µl reactions using 1 µl DNA template, 14.55 µl of molecular grade water, 2 µl 5x OneTaq Standard Reaction Buffer (New England Biolabs), 2 µl 10 mM dNTPs, 0.8 µl 10% BSA, 0.2 µl 10 mM DMSO, 0.2 µl of each 10 µM primer and 0.25 µl OneTaq DNA polymerase (New England Biolabs). The PCR proceeded as follows: initial denaturation of 95°C for 3 min, 40 cycles of denaturation at 94°C for 30 s, annealing at 52°C for 30 s and extension at 68°C for 30 s, followed by a final extension at 68°C for 1 min. Samples were run on 2% agarose gels to confirm the presence of single amplification products of the correct size (213 bp with sequencing primers).

We ran a second PCR on each 213 bp PCR product to attach Illumina Nextera-style fusion primers to the MHC amplicons. The Stiebens *et al.* [52] primers were optimized for 454 sequencing, thus we redesigned them for the Illumina platform. Our forward and reverse fusion primers consisted of the following (5′ to 3′): Nextera-style Illumina adapters, unique 8 bp indices, a 10 bp primer pad, 2 bp linker and the MHC sequencing primers described above. PCRs were performed with unique combinations of forward and reverse fusion primers for MHC amplicons from each individual in a 25 µl reaction, using 4 µl of the PCR product from the first amplification, 6.875 µl molecular grade water, 2.5 µl 5x OneTaq Standard Reaction Buffer (New England Biolabs), 0.5 µl 10 mM dNTPs, 1 µl 10 mM forward fusion primer, 10 µl 1 mM reverse fusion primer and 0.125 µl OneTaq DNA polymerase (New England Biolabs). The PCR was run at an initial denaturation of 95°C for 3 min, 15 cycles of denaturation at 94°C for 30 s, annealing at 52°C for 30 s and extension 68°C for 30 s, followed by a final extension at 68°C for 1 min. Samples were visualized on 2% agarose gels to confirm product size (307 bp including fusion primers) and pooled into three groups based on band intensity (strong, medium and weak). Each pool was cleaned and DNA concentration was quantified, and a final pool was created. We used 1.0 X SpeedBeads (Thermo Fisher Scientific, Waltham, MA) to clean the amplicon pools, which were then quantified with a KAPA qPCR kit following manufacturer's instructions (Roche Sequencing Systems, Pleasanton, CA). The final library pools, each containing roughly equimolar quantities of MHC amplicon from each individual, were sequenced across three Illumina MiSeq 2 × 250 runs, twice at the Oklahoma Medical Research Foundation Clinical Genomics Center and once at the University of Central Florida Genomics and Bioinformatics Cluster. Five individuals were separately amplified and sequenced on the three runs for repeatability to identify possible amplification and sequencing biases. Demultiplexed and adapter-trimmed reads were returned from the sequencing machine and used in downstream analyses.

Paired-end MHC reads were merged using PEAR v. 0.9.11 [58] with default parameters, including a Phred trim quality score of 33. Merged reads were then clustered into MHC alleles using AmpliSAS with the developer's parameter recommendations for Illumina data [59]. We compared maximum allele limits ranging from 1 to 12 alleles. Our minimum amplicon depth was 160 reads and minimum amplicon frequency was 10% for clustering and 3% for filtering. We analysed resulting alleles using Geneious v. 9 [60], removing any allele that was not 162 bp (our fragment size after removing primers), not

recovered in at least two individuals, contained stop codons, or did not have significant BLAST hits with any MHC class Iα sequence.

2.3. Major histocompatibility complex genetic variation

MHC class Iα variability was evaluated separately in alleles recovered from *Ch. mydas* ($n = 98$ alleles) and from *Ca. caretta* ($n = 32$ alleles) in our study. We calculated the average number of alleles per individual in each species and used the nuc.div() and seg.sites() functions from the pegas v. 0.12 [61] and ape v. 5.3 [62] packages in R to calculate nucleotide diversity and number of segregating sites in alleles per species, respectively. We were unable to calculate metrics of heterozygosity because our multi-locus alleles cannot be assigned to specific loci.

2.4. Phylogenetic and network analyses

We used Clustal Omega [63] in Mega v. 7.0.26 [64] to align the sequences. We used MHC sequences from *Gallus gallus* (KF032390.1) and *Tymphanuchus cupido* (KF466478.1) as outgroups and included the eight unique (after removing primer sequence) MHC alleles that were not found in our study and were previously sequenced from a *Ca. caretta* nesting population in Cape Verde, Africa (GenBank IDs: KF021627, KF021629, KF021631–KF021637, KF021639–KF021646, KF021649–KF021651, KF021661, KF021663, and KF021665) [52]. We used PartitionFinder v. 2.1.1 [65] to find the model of evolution that best fit the alignment and reconstructed a Bayesian phylogeny using MrBayes v. 3.2.6 [66] run twice for 1×10^7 generations each, with the first 100 000 iterations discarded as burn-in. Results were visualized in Tracer v. 1.7 [67] to confirm MCMC chain convergence and ensure adequate posterior distribution sampling. We reconstructed a maximum-likelihood phylogeny in RAxML v. 8.2.8 [68] and visualized both phylogenies using the ggtree package [69]. We conducted a haplotype network analysis in PopArt v. 1.7 using the TCS algorithm to visualize allelic frequencies and distributions [70].

2.5. Major histocompatibility complex supertyping

We used discriminant analysis of principal components (DAPC) to identify MHC supertypes based on the physiochemical properties of the amino acid residues in our MHC alignment [71–73]. Using a two-step cross-validation and optimization procedure, we iteratively evaluated and cross-validated the number of principal components to retain at k clusters 3 to 11 using the R package adegenet v. 2.1.2 [74] (electronic supplementary material, methods S1, figures S9–S18).

2.6. Random forest modelling

RF ensemble learning models provide a non-parametric analytical approach to incorporate many explanatory variables and their associations to predict a response variable [75]. For polygenic loci such as MHC, we opted for RF modelling to explore how many explanatory variables of interest, including numerous MHC alleles, might predict disease state in sea turtles. We implemented RF models to predict (i) FP occurrence and (ii) tumour texture, each as a function of the following variables: the presence of each MHC allele, the presence of each MHC supertype, total number of MHC alleles per individual, season (spring, summer, autumn or winter), year, capture location and SCL. Because we had few FP-positive *Ca. caretta* ($n = 4$ out of 88), we conducted these analyses on *Ch. mydas* only. We also corrected imbalance in the response variable of both models by subsampling. For the FP occurrence prediction, we considered any turtle encountered with FP at any point in time to be FP positive. For the tumour texture prediction, we included FP positive *Ch. mydas*, coding individuals as having either rough or smooth FP tumours based on tumour description at time of capture [34]. We did not include the seven individuals with true tumour regression in the RF analyses due to small sample size of this category ($n = 7$). We included data (e.g. SCL, season, year) from the first capture for recaptured turtles, or if applicable, from the capture when FP was observed. Additionally, only individuals that had SCL measurements were included in the analyses ($n = 268$ for the FP occurrence model, $n = 99$ for the tumour texture model). RF analyses were implemented in RStudio using the packages randomForest v. 4.6.14 [76] and caret v. 6.0.86 [77]. We used optimized values for the *mtry* and *ntree* parameters, which dictate the number of variables available to split nodes in each RF decision tree and the total number of trees, respectively. For the final models predicting FP occurrence and tumour texture, the data were randomly separated into 30% test and 70% training datasets. For

FP occurrence, the model was built on the training data with *mtry* = 17 and *ntree* = 10 000. For tumour texture, the final model was built with *mtry* = 50 and *ntree* = 10 000. For both models, a confusion matrix was built and the prediction accuracy of each model was assessed, as well as the relative importance of the predictor variables based on two metrics: mean decrease in accuracy and mean decrease in Gini impurity (see electronic supplementary material, methods S2).

2.7. Relative risk

We conducted risk ratio analyses to explore the MHC-based relative risk of individuals (i) developing FP and (ii) smooth-textured tumours. We included only *Ch. mydas* due to insufficient sampling of FP-positive *Ca. caretta*, and only retained alleles that were found in 10 or more individuals due to low statistical power for small sample sizes [78]. We also assessed relative risk for FP and for smooth tumour texture based on the three MHC supertypes. The seven individuals with true tumour regression were excluded from the tumour texture risk ratio analyses due to small sample size of this category ($n = 7$). Analyses were conducted in RStudio with the package epiR v. 1.0.14 [79] using the epi2by2 function with cohort method and 95% confidence intervals. For any allele for which there was a zero cell (i.e. one of the categories had a count of zero), a Haldane-Anscombe correction was applied [80,81]. Bonferroni correction for multiple comparisons was applied to keep the family-wise error rate at 5% [82].

2.8. Selection analyses

To identify positive selection within the MHC alignment, we implemented HyPhy on the DataMonkey server [83,84], inputting our translated MHC alignment (53 codon alignment of 124 alleles) and Bayesian phylogeny. Model selection was performed within HyPhy to determine which model of DNA evolution best fit the data, and single breakpoint analysis was used to identify intragenic recombination, which can bias selection measurements [83]. Upon detecting significant evidence of recombination, we partitioned the alignment at the recombination breakpoint. For each partition, we identified a model of evolution with PartitionFinder v. 2.1.1 [65] and reconstructed a Bayesian phylogeny using MrBayes v. 3.2.6 [66] with the same methods used for the phylogenetic analysis described previously. We then conducted separate tests of selection on the two partitions and phylogenies, including the following site-specific methods: FEL (Fixed Effects Likelihood), SLAC (Single Likelihood Ancestry Counting) [85], FUBAR (Fast Unconstrained Bayesian AppRoximation) [86] and MEME (Mixed Effects Model of Episodic Diversifying Selection) [87]. We also implemented aBSREL and BUSTED, which are branch and gene-wide tests, respectively, to test for signatures of selection on branches of the MHC phylogeny. aBSREL and BUSTED provide statistical evidence for positive selection on branches of the phylogeny but do not identify individual sites. Significance was inferred at alpha less than or equal to 0.05 or posterior probability greater than or equal to 0.95, as appropriate for the method used.

3. Results

3.1. Major histocompatibility complex sequencing and bioinformatics

We generated robust MHC genotype data for 356 of the 443 juvenile sea turtles we evaluated (268 *Ch. mydas* and 88 *Ca. caretta*) and recovered a maximum of seven MHC alleles per individual (when allowing detection of up to 12 alleles per turtle). Allele counts per turtle ranged from one to seven alleles, with a mean of 3.6 ± 1.4 alleles (electronic supplementary material, figure S1). In total, we recovered 116 unique MHC alleles (corresponding to 99 unique translated amino acid alleles), of which 15 were identical to previously identified alleles in Cape Verde *Ca. caretta* [52]. Among the samples amplified and sequenced independently, four returned identical results while one differed slightly between sequencing runs, with five alleles identified in run 1 and four of those same five alleles identified in run 2, when total sample read depth was lower (electronic supplementary material, table S1). Eighty-four alleles occurred only in *Ch. mydas* and six occurred only in Florida-sampled *Ca. caretta*. Eleven alleles were shared by *Ch. mydas* and *Ca. caretta* from Florida, 12 alleles were shared by Florida and Cape Verde *Ca. caretta*, and three alleles were shared by *Ch. mydas*, Florida *Ca. caretta* and Cape Verde *Ca. caretta*. Among MHC-genotyped *Ch. mydas*, 106/268 (39.6%) individuals in our dataset had FP at the time they were sampled. FP occurrence was much lower in *Ca. caretta*, with only 4/88 (4.5%) of individuals manifesting FP at the time of sampling.

Table 1. Estimates of MHC genetic diversity for alleles recovered in *Ch. mydas* and *Ca. caretta*, including turtle sample sizes (N), allele sample size (n), average number of alleles observed per individual, segregating sites over 162 bp and nucleotide diversity.

species	turtles sampled (N)	alleles sampled (n)	average number of alleles observed (s.d.)	segregating sites	nucleotide diversity
Ch. mydas	268	98	3.5 ± 1.4	106 (65.43%)	0.201021837
Ca. caretta	88	32	3.9 ± 1.5	95 (58.64%)	0.2347795

3.2. Major histocompatibility complex genetic variation

Among MHC alleles recovered from *Ch. mydas*, there were 106 segregating sites out of the 162 total sequenced nucleotides (65.4%) and nucleotide diversity was 0.20. Similarly, among MHC alleles recovered from *Ca. caretta* there were 95 segregating sites out of 162 (58.6%) and nucleotide diversity was 0.23 (table 1).

3.3. Phylogenetic reconstruction, major histocompatibility complex supertyping and haplotype network analysis

We identified three well-supported clades of MHC alleles (figure 2; electronic supplementary material, figure S2). DAPC clustered the 124 alleles into three distinct supertypes (electronic supplementary material figures S10A, S10B), which correspond precisely to these three clades. The supertype A clade had not previously been identified, whereas alleles from supertype B and C clades were recovered in the previous study of *Ca. caretta* MHC [52]. Alleles did not cluster by species (colours), by FP status (asterisks), or by geographic location (Florida versus Cape Verde) (figure 2). A majority of the 116 alleles recovered in this study were found in only a few individuals, but some occurred at high frequency, particularly within supertype B (figure 3). All alleles that occurred in both species were primarily recovered in either *Ch. mydas* or *Ca. caretta*, and were never common in both species (figure 3).

3.4. Random forest modelling

The RF model predicting *Ch. mydas* FP occurrence had an out-of-bag error rate of 37.04% and prediction accuracy of 67.38%. Variables that had the highest relative importance in predicting FP were location, SCL, year, and season. Individual MHC alleles showed lower relative importance, although allele Chmy49 and allele count had the highest relative importance of any MHC variable based on mean decrease accuracy and mean decrease Gini impurity, respectively (figure 4). The RF model predicting *Ch. mydas* FP tumour texture had an out-of-bag error rate of 26.67% and prediction accuracy of 66.67%. The predictor variables with the highest relative importance based on mean decrease accuracy and mean decrease Gini impurity included year, SCL, allele count, and MHC alleles Chmy04 and Chmy80 (figure 5).

3.5. Relative risk

Chelonia mydas with allele Chmy13 had a significantly elevated risk ratio for having FP (RR = 1.74; 95% CI = 1.13–2.68; electronic supplementary material, figure S5), although this was not significant after Bonferroni correction (RR = 1.74; 99.8% CI = 0.885–3.43). Among FP positive *Ch. mydas*, individuals with alleles Chmy04 had a significantly elevated risk ratio for having tumours with smooth texture (Chmy04: RR = 2.28, 95% CI = 1.08–4.81; electronic supplementary material, figure S6), but this was not significant after Bonferroni correction (RR = 2.28; 99.9% CI = 0.851–6.09).

Chelonia mydas with MHC supertype B had a significantly decreased risk for having FP (RR = 0.731, 95% CI = 0.544–0.982; electronic supplementary material, figure S7), but this was not significant after Bonferroni correction (RR = 0.731, 98.3% CI 0.510–1.05). There were no significant associations between smooth tumour texture and MHC supertype (electronic supplementary material, figure S8).

3.6. Selection analyses

Across the 124 alleles, seven codons in the 53 codon alignment evolved under positive selection based on at least one site-based method (table 2; electronic supplementary material, figure S3) and 4/4 site-based

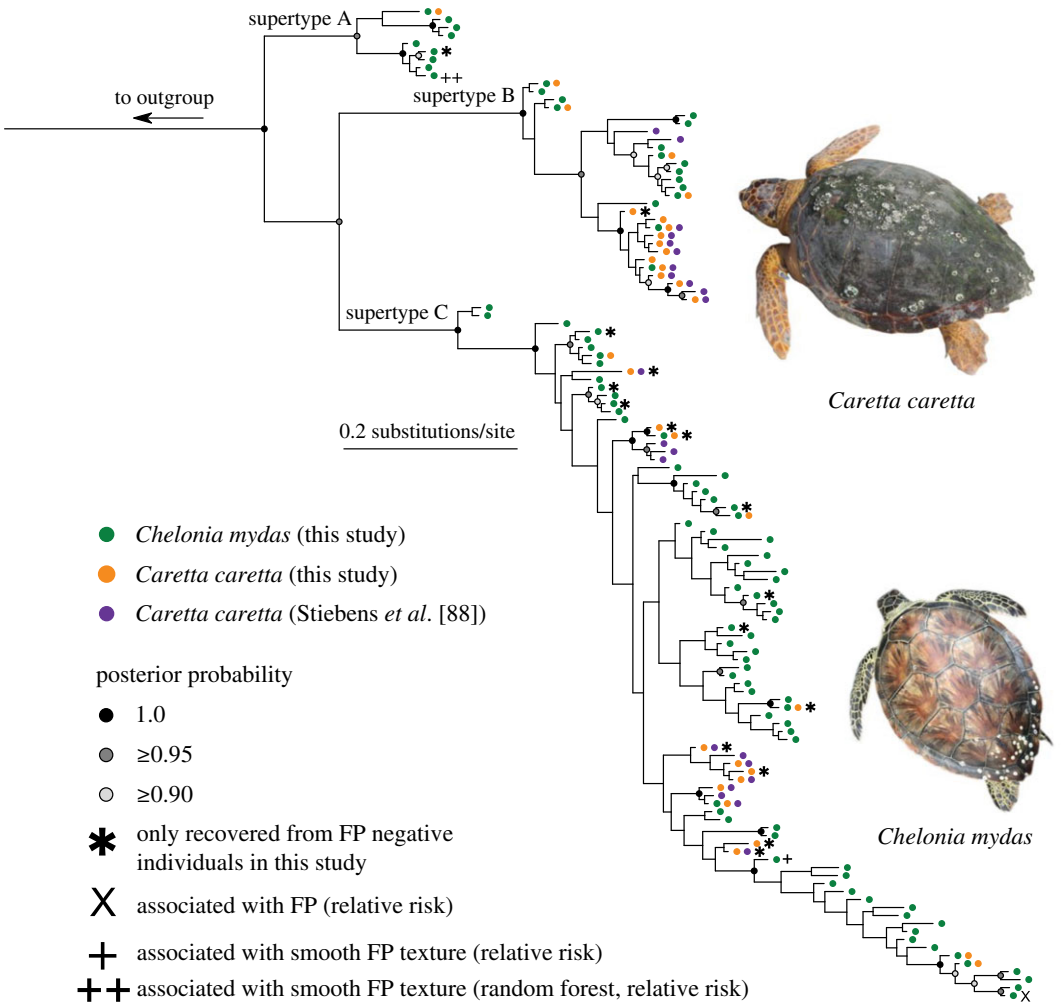

Figure 2. Bayesian phylogeny of 124 alleles of exon 2 (162 bp) of the Iα MHC in *Ch. mydas* and *Ca. caretta* (116 of which were recovered from turtles sampled in this study from the central Florida Atlantic coast). Posterior probabilities greater than 0.90 are shown and supertype group membership is denoted on interior branch. Asterisk denotes alleles recovered in FP negative turtles. 'X' denotes alleles significantly with FP in relative risk analysis. Single cross symbol denotes alleles associated with smooth tumour texture per relative risk analysis; double cross symbol denotes alleles associated with smooth tumour texture per random forest modelling and relative risk analysis.

methods identified codon 51 evolving under positive selection. BUSTED detected episodic diversifying selection in at least one site on at least one branch of the phylogeny, whereas aBSREL did not detect any evidence of episodic diversifying selection in the phylogeny. Across our alleles, six unique amino acids occur at codon 51: aspartic acid, glutamic acid, glutamine, arginine, tryptophan and tyrosine. Some clades in our phylogeny include a wide variety of these six amino acids at position 51, whereas other clades have only one or two amino acids (electronic supplementary material, figure S4). The allele not significantly associated with FP occurrence in the relative risk analyses, Chmy13, has a tryptophan at codon 51, which is amphipathic. The alleles weakly associated with smooth tumour texture from the RF analyses have arginine (Chmy04), and tryptophan (Chmy80) at codon 51, which are charged and amphipathic, respectively.

4. Discussion

Our study provides the first characterization of MHC immunogenetic diversity in any life stage of *Ch. mydas* and the first in juvenile *Ca. caretta*. We recovered high MHC class Iα polymorphism in both species based on sequence diversity and number of recovered alleles. Low immunogenetic diversity following population bottlenecks has been documented in amphibians [89], birds [90] and non-avian reptiles [53]; however, despite historical reductions in *Ch. mydas* population sizes [31] and threats to

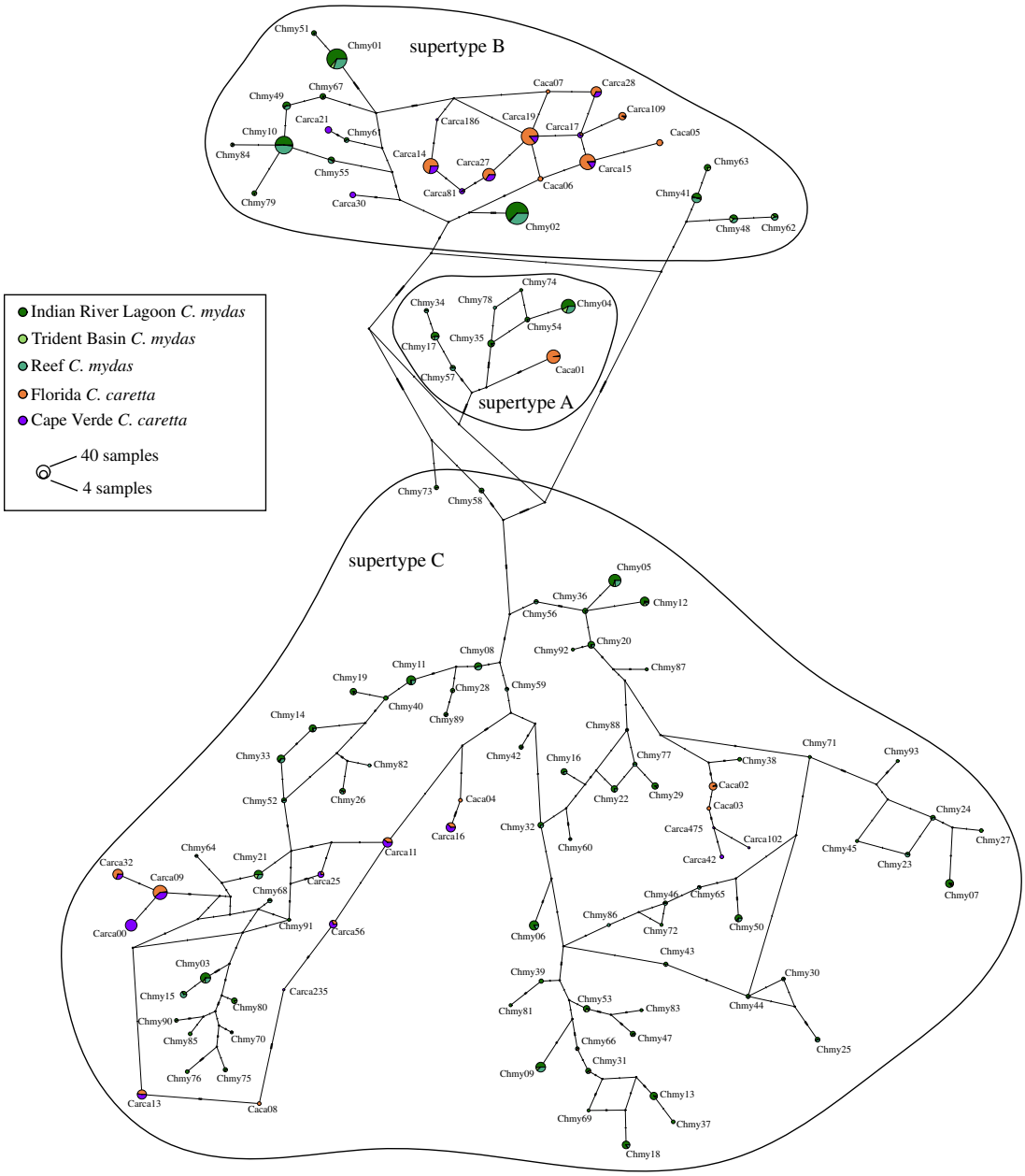

Figure 3. Haplotype network of 124 class I exon 2α (162 bp) MHC alleles recovered in *Ch. mydas* and *Ca. caretta* juveniles. Circle size in proportional to overall allele frequency, and alleles are coloured proportionally according to species and field study location (Florida or Cape Verde for *Ca. caretta*; IRL, Trident or Reef for *Ch. mydas*). Supertypes are denoted with black outlines. Allele frequencies for Cape Verde *Ca. caretta* from [88] and C. Eizaguirre (personal communication).

Ca. caretta [91], we found no evidence of low immunogenetic diversity in sea turtles. We found no significant associations between MHC alleles and FP tumour development or tumour texture. Because standing immunogenetic variation is critical for the survival of disease-threatened organisms, as it allows ongoing adaptation to changing pathogen pressures [16], we were surprised to find only minimal MHC-disease associations in our study. However, the high number of recovered alleles made sample sizes small for most individual allele-disease associations, and we hope future studies will continue to characterize MHC variation in the context of FP as we suspect larger allele sampling could reveal stronger relationships. Alternatively, MHC may not function in sea turtles as documented in other taxa, and characterizing non-MHC immune genes and immune function are important priorities given the threat posed by FP, especially in the severely affected *Ch. mydas* [26,34] and in juveniles newly recruited to neritic waters [92]. Recent functional immune studies demonstrate reduced natural killer cell response in *Ch. mydas* with FP [39] and reduced phagocytosis in individuals

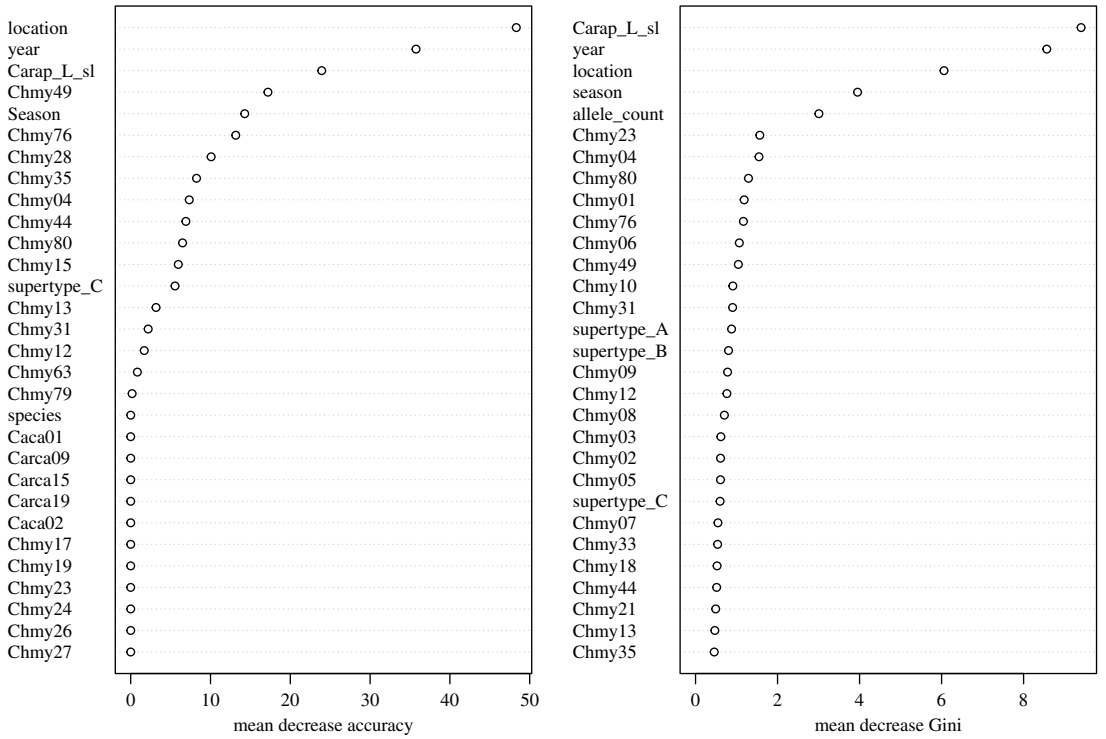

Figure 4. Mean decrease in accuracy (*a*) and Gini impurity (*b*) for random forest model relating FP occurrence in *Ch. mydas* from the central Florida Atlantic coast to MHC genetic diversity predictors.

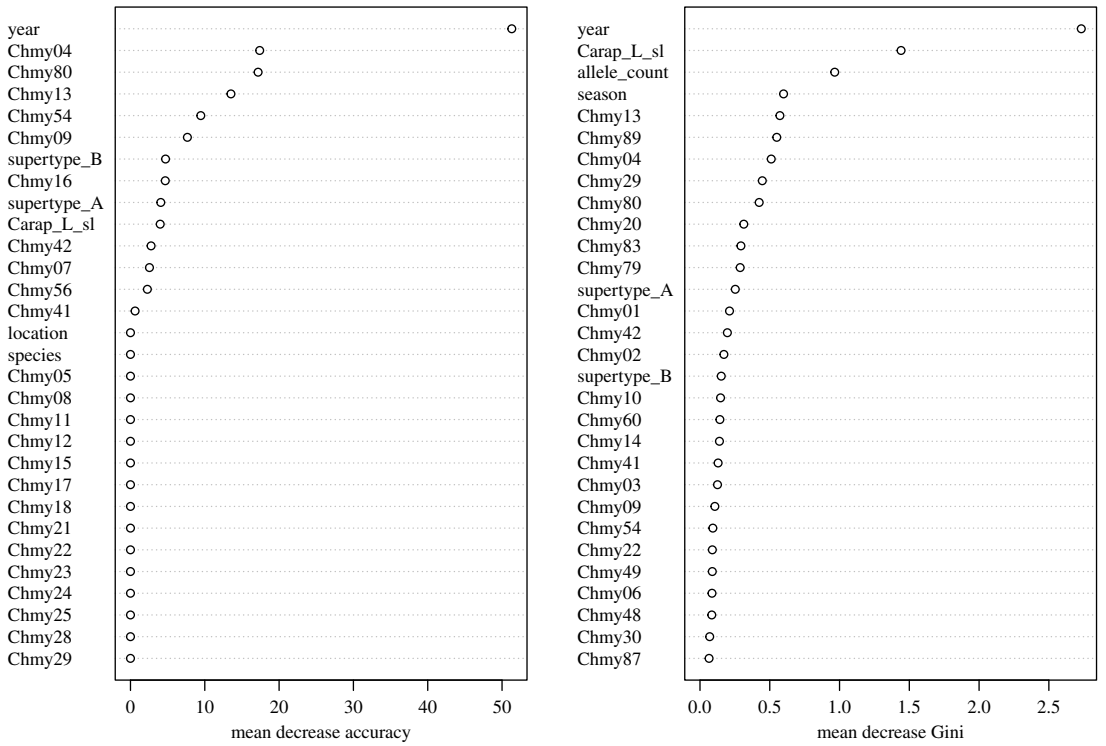

Figure 5. Mean decrease in accuracy (*a*) and Gini impurity (*b*) for RF model relating tumour texture in *Ch. mydas* from the central Florida Atlantic coast to MHC genetic diversity predictors.

in degraded habitat, regardless of FP status [42]. Additionally, several gene expression studies in *Ch. mydas* indicate that FP is associated with changes in immune gene expression, including upregulated immune checkpoint molecules in tumours [43], heightened T-lymphocyte activity in early-stage tumours and distinct expression patterns in internal versus external tumours [44],

Table 2. HyPhy branch- and site-specific tests of positive selection in the codon alignment of exon 2 (PBR) of MHC class Iα in *Ch. mydas* and *Ca. caretta*. Evidence of positive selection at each codon position is denoted with an X, with method and statistical criteria specified.

		codon position						
method	statistical cut off	2	3	10	18	36	42	51
aBSREL	$p \leq 0.05$	no evidence of episodic diversifying selection across phylogeny						
FEL	$p \leq 0.05$	X					X	X
FUBAR	posterior probability ≥ 0.95			X	X			X
MEME	$p \leq 0.05$	X	X	X		X		X
SLAC	$p \leq 0.05$							X
BUSTED	$p \leq 0.05$	gene-wide episodic diversifying selection on at least one branch						

upregulated tumour inhibition transcripts in FP-afflicted turtles [45] and alteration of signalling pathways in FP tumours that have also been implicated in human cancers [46]. Together, these studies demonstrate the importance of understanding the immune system's role in FP, and we advocate for the continued evaluation of sea turtle immunogenomic repertoires using gene expression analysis, functional immune assays and immune gene characterization.

Our RF modelling had low predictive power overall (67.38% for FP development and 66.67% for smooth tumour texture). MHC allele Chmy13 and MHC supertype B were associated with FP risk in the relative risk analyses, but neither association was significant after Bonferroni correction. For tumour texture, MHC allele Chmy04 was the second highest ranked variable for decrease in mean accuracy in the RF model and was associated with an increased risk of smooth tumour texture in the relative risk analysis, although this was not significant after Bonferroni correction. Further sampling of Chmy04 and the other weakly disease-linked MHC variables identified here will be important for confirming any associations with FP development and tumour texture. In a recent study of host and viral gene expression in *Ch. mydas*, Blackburn *et al*. [43] found that two tumours with the highest levels of ChHV5 transcripts (suggesting tumour growth) had smooth texture and altered pigmentation. By contrast, smooth tumour texture was anecdotally linked to tumour regression in juvenile *Ch. mydas* sampled in the IRL [34]. While we cannot conclusively link tumour texture to either FP progression or regression, we suggest that tumour appearance and its relation to host immune function, tumour gene expression, and disease outcome is an area of exploration for future studies. Moreover, immunogenetic and functional immune studies in sea turtles with true regression (i.e. shrinking or disappearance of tumours from initial capture to subsequent recapture) may also provide insight into the mechanisms behind the variable outcomes of FP. Given the current modest support linking MHC and FP, and the complexity of the vertebrate immune system, immunogenetic associations with FP may largely be driven by other immune loci and/or immunogenetic–environmental interactions. Based on previous transcriptome-wide studies in sea turtles [43–46,93], gene expression studies could be especially illuminating in evaluating the role of MHC expression relative to tumour development, where MHC expression may be a better predictor of FP status than the presence or absence of specific alleles. FP is rarely documented in species other than *Ch. mydas*, making species-level comparisons of disease incidence difficult. We suggest that sampling FP-positive *Ca. caretta* should be a priority in sea turtle disease studies to provide insight into host differences that may translate into different rates of juvenile FP documented between species at our field sites. Despite the limitations of our disease analyses, our study provides a valuable survey of MHC diversity in two sea turtle species, and a first step in understanding potential relationships between immunogenetic variation and disease occurrence in sea turtles.

We detected high MHC class Iα polymorphism in both juvenile *Ch. mydas* and *Ca. caretta*, bringing the number of unique alleles identified in sea turtles to 124 [52,88]. In both species, the percentage of segregating sites was over 50%. However, this polymorphism is potentially overestimated, as the alleles we recovered come from multiple unidentified loci. By comparison, studies of Testudines that were able to assign MHC class I alleles to loci found that across 18 populations of Gopher tortoise (*Gopherus polyphemus*) at MHC class I exon 3, there were 13% segregating sites and nucleotide

diversity was 0.03 [53]; furthermore, in a population of Diamondback terrapins (*Malaclemys terrapin*), the MHC class I locus was fixed for a single allele [50]. By contrast, our conservative criteria for retaining alleles means we are probably underestimating total alleles, and additional sea turtle MHC studies will almost certainly reveal further MHC class Iα diversity. Also, given documented MHC copy number variation among individuals in other taxa [90,94], including in reptiles (e.g. birds) with up to 33 loci [95], further sea turtle MHC sampling could find that the maximum number of alleles per individual may exceed seven. However, the exploration of MHC genomic structure in sea turtles using new genomic resources such as well-annotated assemblies of the *Ch. mydas* genome (rCheMyd1; RefSeq assembly accession GCF_015237465.1) and implementation of bioinformatics approaches [96] will be critical for resolving the extent of MHC copy number variation in sea turtles.

We found both sequence and allelic diversity patterns that are generally consistent with MHC class Iα evolving adaptively via balancing selection to maintain polymorphism [97]. In studies of MHC, patterns consistent with balancing selection are usually interpreted in the context of pathogen-mediated balancing selection, where pathogen pressure selects for high levels of MHC polymorphism via several non-mutually exclusive selective processes, including heterozygote advantage, frequency-dependent selection (or rare allele advantage) and fluctuating selection [12,16], although distinguishing between the different mechanisms of pathogen-mediated balancing selection is very difficult [98].

At the sequence level, we detected some evidence of positive selection at seven MHC codons, and all four site-specific tests identified codon 51 as evolving under positive selection. An increased rate of non-synonymous relative to synonymous substitutions at MHC peptide-binding residues is consistent with pathogen-mediated selection [99]. While codon 51 is not homologous to a known peptide-binding residue when aligned to the human reference, our results suggest it is the most important target of adaptive evolution in sea turtle MHC class Iα and may play an important role in reptilian MHC pathogen-binding. Across our sampled alleles, six different amino acids with distinct-binding abilities occurred at codon 51, which could be indicative of variable pathogen-binding ability at this residue across MHC alleles, perhaps driven by fluctuating selection or changing pathogen pressures. However, unless stronger relationships between FP and specific amino acid changes in MHC alleles are found, we cannot robustly link these signatures of positive molecular selection or amino acid variation at codon 51 to pathogen pressure. Numerous studies of MHC class II evolution evaluate specific codons under selection and find consistent amino acid changes and associations with disease [17,20,100,101], but to our knowledge, only one other study has established similar codon-disease associations in reptilian class I loci [49]. Thus, we encourage similar studies across reptilian taxa to provide a better framework for drivers of MHC class I adaptive evolution and to identify common targets of pathogen-mediated selection.

Previous studies suggest that individuals with intermediate numbers of MHC alleles may have greater fitness compared with those with maximized heterozygosity [102,103], where high MHC diversity may be selectively advantageous for pathogen binding but is disadvantageous because it leads to greater T-cell repertoire depletion to prevent autoimmunity [98,104]. While the average number of alleles we recovered per turtle is generally consistent with this pattern of intermediate allele numbers, we did not find statistical support for an association between FP and number of alleles in sea turtles. Further, we caution that PCR amplification biases often affect estimates of MHC allele count [105,106], limiting confidence in estimates of allele counts per individual.

The total number of alleles we recovered from both species is high, which is consistent with expectations that balancing selection will maintain high levels of allelic polymorphism. However, the aggregations of *Ch. mydas* and *Ca. caretta* juveniles that recruit to neritic foraging waters after their early oceanic stage [34,55] represent mixed genetic stocks from multiple source rookeries [107] which may be driving the sheer number of recovered MHC alleles in our study. Only a few dozen mtDNA haplotypes have been recovered from the entire northwest Atlantic region, most differing from each other by a single nucleotide [108], suggesting that the high MHC polymorphism we recovered is not necessarily caused by sampling particularly diverse genetic lineages. However, we caution against over-interpretation given that mitochondrial and MHC loci are subject to different demographic processes; evaluation of the molecular evolution of numerous nuclear loci and assignment of individual MHC alleles to loci are needed before we can robustly quantify the genetic diversity present within our study area or describe the evolutionary forces that shaped it. Finally, gene flow between source populations with different levels of local MHC polymorphism may also be inflating MHC diversity estimates and obscuring potential associations with FP.

The pattern of shared MHC alleles we found in *Ch. mydas* and *Ca. caretta* is also consistent with expectations under balancing selection. The three clades of alleles we recovered did not cluster by

species; instead 14 identical alleles occurred in both species (including alleles sampled from Cape Verde *Ca. caretta* [52]), and many *Ch. mydas* and *Ca. caretta* alleles shared closer evolutionary histories with each other than with other alleles from the same species (figure 2). We note with interest that this allele sharing spans across the subfamilies Carettinae and Cheloniinae and that shared MHC polymorphism between genera or higher taxonomic ranks is only rarely documented [109–111]. Shared alleles are potentially explained by trans-species polymorphism [112], wherein standing ancestral MHC polymorphism is maintained through speciation due to incomplete lineage sorting [113] and is subsequently preserved by balancing selection in the descendant species [114]. Alternatively, shared alleles among species may also originate through hybridization; in the case of MHC, novel allele advantage is thought to promote adaptive introgression [115,116]. While *Ch. mydas* and *Ca. caretta* speciated approximately 63 million years ago [117], hybridization with viable offspring occurs between Cheloniidae species [118,119]. Furthermore, *Ch. mydas* × *Ca. caretta* hybrids have been documented [120], including a first generation hybrid in our TB field site [121]. We suggest that introgression between *Ch. mydas* and *Ca. caretta* could explain at least part of this pattern. However, shared alleles between species may also arise from convergent evolution or from nucleotide changes that result in reversions to the ancestral state, and distinguishing the mechanisms by which shared alleles arise in related taxa is difficult in practice [113]. Finally, we acknowledge that sea turtle MHC polymorphism is probably shaped by multiple factors and selective pressures working simultaneously, and that disentangling them will require focused sampling across time and populations, as well as sampling neutral marker data for comparison with MHC evolution. We note that balancing selection also encompasses other selective pressures such as assortative mating and maternal–fetal interactions that may work to maintain MHC polymorphism [97]. While testing for these phenomena is beyond the scope of this study, they may be valid avenues of research given the limited evidence we found for a relationship between sea turtle MHC and FP.

Reptile immune systems are relatively understudied by comparison with birds and mammals [51]. Our study underscores this need for more studies of reptile immunogenetics: with such high numbers of MHC alleles, we lack the sampling depth at each allele to robustly explain FP status. Furthermore, the innate immune system is postulated to be more robust than the acquired immune system in reptiles due to life history and ectothermy [122,123], and we suggest that investigations into non-MHC immune genes and genes associated with the innate immune system (e.g. natural antibodies [124]) may be fruitful next steps for understanding FP in sea turtles, and more broadly in understanding how immunogenetics moderates disease in reptiles.

Coastal habitats are an important incubator of genetic diversity in sea turtles [107], and our study suggests they may also be a haven of immunogenetic diversity, although similar studies from other regions are necessary to determine whether MHC diversity is equally high in other sea turtle aggregations and populations. Juvenile sea turtles face numerous threats, including nutrient pollution in foraging grounds [125], historical population contractions from overexploitation [31], and disease [36]. Disease is a particular problem in coastal sea turtle foraging habitat, where pathogen-naive juveniles are proposed to be initially exposed to the ChHV5 virus after recruitment from oceanic waters [92] and where pollution may exacerbate disease [126]. Standing levels of immunogenetic variation at the coastal juvenile life stage may very well be a deciding factor in survival and future fitness. We advise that monitoring the immunogenetic diversity of both source populations and juvenile aggregations is important given that delayed sexual maturity and long generation intervals in sea turtles may limit their response to environmental pressures (e.g. ChHV5), warranting conservation measures at multiple life stages [127]. Future studies characterizing immunogenetic diversity in other life stages and species of sea turtles should be conducted to improve our understanding of sea turtle immune systems and that of reptiles more broadly. Reptilian immune systems are poorly studied relative to other vertebrate taxa [51], and although expression changes in immune-related genes have been consistently linked to FP tumour development and sea turtle outcome [43–46], the roles of the innate and acquired immune systems in fighting disease remain open questions in reptile biology [128]. Our study demonstrates the extent of MHC polymorphism that has evolved in sea turtles despite an apparently weak association with the FP disease and illustrates that the study of reptilian MHC can broaden our understanding of how the vertebrate immune system evolves and functions.

Ethics. All samples were collected under National Marine Fisheries Service permit no. 19508 and Florida Marine Turtle Permits 231 and 225 (and all associated predecessors), as well as approved institutional animal care and use committee protocols.

Data accessibility. Data and relevant code for this study are stored on GitHub: https://github.com/katherinermartin/Martin_et_al_RSOS_2021 and archived within the Zenodo repository: https://doi.org/10.5281/zenodo.5703775 [129]. The sequence data are available in GenBank, accession numbers OK135205–OK135305. The data are provided in the electronic supplementary material [130].

Authors' contributions. K.R.M.: data curation, formal analysis, investigation, project administration, writing—original draft, writing—review & editing; K.L.M.: conceptualization, funding acquisition, project administration, resources, supervision, writing—review & editing; A.E.S.: conceptualization, funding acquisition, methodology, project administration, resources, supervision, writing—review & editing

All authors gave final approval for publication and agreed to be held accountable for the work performed therein.

Competing interests. We declare we have no competing interests.

Funding. This work was supported by the Florida Sea Turtle License Plate Program which is funded by the proceeds of the Florida Sea Turtle License Plate (award no. 18-033R, 2018–19). Article processing charges were provided in part by the UCF College of Graduate Studies Open Access Publishing Fund.

Acknowledgements. We are grateful to the many members of the MTRG over the last 40 years for their dedication to collecting and cataloguing samples; M. Lawrance, E. Sutton, and A. Trujillo for their help in primer design, DNA extraction, and generating pilot data; R. Fitak for assistance with statistical analysis; and V. Urgiles for help with figures and maps. We also thank members of the Savage lab, MTRG, and several anonymous reviewers for their feedback on earlier versions of this manuscript.

References

1. Daszak P, Cunningham AA, Hyatt AD. 2001 Anthropogenic environmental change and the emergence of infectious diseases in wildlife. *Acta Trop.* **78**, 103–116. (doi:10.1016/s0001-706x(00)00179-0)
2. Daszak P, Cunningham AA, Hyatt AD. 2000 Emerging infectious diseases of wildlife—threats to biodiversity and human health. *Science* **287**, 443–449. (doi:10.1126/science.287.5452.443)
3. Gallana M, Ryser-Degiorgis MP, Wahli T, Segner H. 2013 Climate change and infectious diseases of wildlife: altered interactions between pathogens, vectors and hosts. *Curr. Zool.* **59**, 427–437. (doi:10.1093/czoolo/59.3.427)
4. Zamora-Vilchis I, Williams SE, Johnson CN. 2012 Environmental temperature affects prevalence of blood parasites of birds on an elevation gradient: implications for disease in a warming climate. *PLoS ONE* **7**, e39208. (doi:10.1371/journal.pone.0039208)
5. Martin LB, Hopkins WA, Mydlarz LD, Rohr JR. 2010 The effects of anthropogenic global changes on immune functions and disease resistance. *Ann. NY Acad. Sci.* **1195**, 129–148. (doi:10.1111/j.1749-6632.2010.05454.x)
6. Altizer S, Ostfeld RS, Johnson PTJ, Kutz S, Harvell CD. 2013 Climate change and infectious diseases: from evidence to a predictive framework. *Science* **341**, 514–519. (doi:10.1126/science.1239401)
7. Böhm M, Cook D, Ma H, Davidson AD, García A, Tapley B, Pearce-Kelly P, Carr J. 2016 Hot and bothered: using trait-based approaches to assess climate change vulnerability in reptiles. *Biol. Conserv.* **204**, 32–41. (doi:10.1016/j.biocon.2016.06.002)
8. Goessling JM, Koler SA, Overman BD, Hiltbold EM, Guyer C, Mendonça MT. 2017 Lag of immunity across seasonal acclimation states in gopher tortoises (*Gopherus polyphemus*). *J. Exp. Zool. Part A Ecol. Integr. Physiol.* **327**, 235–242. (doi:10.1002/jez.2069)
9. Raffel TR, Rohr JR, Kiesecker JM, Hudson PJ. 2006 Negative effects of changing temperature on amphibian immunity under field conditions. *Funct. Ecol.* **20**, 819–828. (doi:10.1111/j.1365-2435.2006.01159.x)
10. Scheele BC *et al.* 2017 After the epidemic: ongoing declines, stabilizations and recoveries in amphibians afflicted by chytridiomycosis. *Biol. Conserv.* **206**, 37–46. (doi:10.1016/j.biocon.2016.12.010)
11. Schumacher J. 2006 Selected infectious diseases of wild reptiles and amphibians. *J. Exot. Pet Med.* **15**, 18–24. (doi:10.1053/j.jepm.2005.11.004)
12. Bernatchez L, Landry C. 2003 MHC studies in nonmodel vertebrates: what have we learned about natural selection in 15 years? *J. Evol. Biol.* **16**, 363–377. (doi:doi:10.1046/j.1420-9101.2003.00531.x)
13. Simpson E. 1988 Function of the MHC. *Immunology* **64**, 27–30.
14. Murphy K, Weaver C. 2017 *Janeway's immunobiology*, 9th edn. New York, NY: Garland Science/Taylor & Francis Group, LLC.
15. Malissen M, Malissen B, Jordan BR. 1982 Exon/intron organization and complete nucleotide sequence of an HLA gene. *Proc. Natl Acad. Sci. USA* **79**, 893–897. (doi:10.1073/pnas.79.3.893)
16. Sommer S. 2005 The importance of immune gene variability (MHC) in evolutionary ecology and conservation. *Front. Zool.* **2**, 1–18. (doi:10.1186/1742-9994-2-16)
17. Savage AE, Zamudio KR. 2011 MHC genotypes associate with resistance to a frog-killing fungus. *Proc. Natl Acad. Sci. USA* **108**, 16 705–16 710. (doi:10.1073/pnas.1106893108)
18. Sepil I, Lachish S, Hinks AE, Sheldon BC. 2013 Mhc supertypes confer both qualitative and quantitative resistance to avian malaria infections in a wild bird population. *Proc. R. Soc. B* **280**, 20130134. (doi:10.1098/rspb.2013.0134)
19. Siddle HV, Kreiss A, Eldridge MDB, Noonan E, Clarke CJ, Pyecroft S, Woods GM, Belov K. 2007 Transmission of a fatal clonal tumor by biting occurs due to depleted MHC diversity in a threatened carnivorous marsupial. *Proc. Natl Acad. Sci. USA* **104**, 16 221–16 226. (doi:10.1073/pnas.0704580104)
20. Du M, Chen SL, Liu YH, Liu Y, Yang JF. 2011 MHC polymorphism and disease resistance to vibrio anguillarum in 8 families of half-smooth tongue sole (*Cynoglossus semilaevis*). *BMC Genet.* **12**, 1–11. (doi:10.1186/1471-2156-12-78)
21. Herbst LH. 1994 Fibropapillomatosis of marine turtles. *Annu. Rev. Fish Dis.* **4**, 389–425. (doi:10.1016/0959-8030(94)90037-X)
22. Herbst LH, Jacobson ER, Moretti R, Brown T, Sundberg JP, Klein PA. 1995 Experimental transmission of green turtle fibropapillomatosis using cell-free tumor extracts. *Dis. Aquat. Organ.* **22**, 1–12. (doi:10.3354/dao022001)
23. Lawrance MF, Mansfield KL, Sutton E, Savage AE. 2018 Molecular evolution of fibropapilloma-associated herpesviruses infecting juvenile green and loggerhead sea turtles. *Virology* **521**, 190–197. (doi:10.1016/j.virol.2018.06.012)
24. Huerta P, Pineda H, Aguirre A, Spraker T, Sarti L, Barragán A. 2002 First confirmed case of fibropapilloma in a Leatherback turtle (*Dermochelys coriacea*). In *Proc. of the 20th Annu. Symp. on Sea Turtle Biology and Conservation*, *29 February–4 March 2000*, *Orlando, Florida, USA*, p. 193. U.S. Department of Commerce, National Oceanographic and Atmospheric Administration, National Marine Fisheries Service, Miami, FL.
25. Aguirre AA, Spraker TR, Chaves A, Du Toit L, Eure W, Balazs GH. 1999 Pathology of fibropapillomatosis in olive ridley turtles *Lepidochelys olivacea* nesting in Costa Rica.

J. Aquat. Anim. Health **11**, 283–289. (doi:10.1577/1548-8667(1999)011<0283:POFIOR>2.0.CO;2)

26. Jones K, Ariel E, Burgess G, Read M. 2016 A review of fibropapillomatosis in green turtles (*Chelonia mydas*). *Vet. J.* **212**, 48–57. (doi:10.1016/j.tvjl.2015.10.041)
27. Barragán AR, Sarti-Martínez L. 1994 A possible case of fibropapilloma in Kemp's ridley turtle (*Lepidochelys kempii*). *Mar. Turt. Newsl.* **67**, 27.
28. D'Amato AF, Moraes-Neto M. 2000 First documentation of fibropapillomas verified by histopathology in *Eretmochelys imbricata*. *Mar. Turt. Newsl.* **89**, 12–13.
29. Limpus CJ, Couper PJ, Couper KLD. 1992 Crab Island revisted: reassessment of the world's largest flatback turtle rookery after twelve years. *Mem. Queensl. Museum* **33**, 277–289.
30. Bolten AB. 2003 Variation in sea turtle life history patterns: neritic vs oceanic developmental stages. In *The biology of sea turtles* (eds PL Lutz, JA Musick, JW Wyneken), pp. 243–257. Boca Raton, FL: CRC Press.
31. Seminoff JA *et al*. 2015 Status review of the green turtle (*Chelonia mydas*) under the Endangered Species Act. NOAA Technical Memorandum, NOAA-NMFS-SWFSC-539.
32. Lackovich JK *et al*. 1999 Association of herpesvirus with fibropapillomatosis of the green turtle *Chelonia mydas* and the loggerhead turtle *Caretta caretta* in Florida. *Dis. Aquat. Organ.* **37**, 89–97. (doi:10.3354/dao037089)
33. Ehrhart LM, Mansfield KL, Redfoot WE, Gorham J, Weege ST, Provancha J. 2016 Prevalence and trends in fibropapillomatosis in green turtles on Florida's Atlantic Coast. In *Proc. of the 2015 Int. Summit on Fibropapillomatosis: Global Status, Trends, and Population Impacts* (eds ST Hargrove, TM Work, S Brunson, AM Foley, GH Balazs), pp. 15–21. Washington, DC: U.S. Dep. Commer. NOAA Tech. Memo., NOAA-TM-NMFS-PIFSC-54. (doi:10.7289/V5/TM-PIFSC-54)
34. Hirama S, Ehrhart LM. 2007 Description, prevalence and severity of green turtle fibropapillomatosis in three developmental habitats on the east coast of Florida. *Florida Sci.* **70**, 435–448.
35. Guimarães SM, Gitirana HM, Wanderley AV, Monteiro-Neto C, Lobo-Hajdu G. 2013 Evidence of regression of fibropapillomas in juvenile green turtles *Chelonia mydas* caught in Niterói, southeast Brazil. *Dis. Aquat. Organ.* **102**, 243–247. (doi:10.3354/dao02542)
36. Hargrove S, Work TM, Brunson S, Foley AM, Balazs GH. 2016 *Proc. of the 2015 Int. Summit of Fibropapillomatosis: Global Status, Trends, and Population Impacts*. U.S. Department of Commerce, NOAA Technical Memorandum, NOAA-TM-NMFS-PIFSC-54. (doi:10.7289/V5/TM-PIFSC-54)
37. Cray C, Varella R, Bossart GD, Lutz P. 2001 Altered in vitro immune responses in green turtles (*Chelonia mydas*) with fibropapillomatosis. *J. Zoo Wildl. Med.* **32**, 436–440. (doi:10.1638/1042-7260(2001)032[0436:AIVIRI]2.0.CO;2)
38. Work TM, Rameyer RA, Balazs GH, Cray C, Chang SP. 2001 Immune status of free-ranging green turtles with fibropapillomatosis from Hawaii. *J. Wildl. Dis.* **37**, 574–581. (doi:10.7589/0090-3558-37.3.574)
39. Perrault JR *et al*. 2021 Insights on immune function in free-ranging green sea turtles (*Chelonia mydas*) with and without fibropapillomatosis. *Animals* **11**, 1–20. (doi:10.3390/ani11030861)
40. da Silva CC, Klein RD, Barcarolli IF, Bianchini A. 2016 Metal contamination as a possible etiology of fibropapillomatosis in juvenile female green sea turtles *Chelonia mydas* from the southern Atlantic Ocean. *Aquat. Toxicol.* **170**, 42–51. (doi:10.1016/j.aquatox.2015.11.007)
41. Foley AM, Schroeder BA, Redlow AE, Fick-Child KJ, Teas WG. 2005 Fibropapillomatosis in stranded green turtles (*Chelonia Mydas*) from the Eastern United States (1980–98): trends and associations with environmental factors. *J. Wildl. Dis.* **41**, 29–41. (doi:10.7589/0090-3558-41.1.29)
42. Sposato P, Keating P, Lutz PL, Milton SL. 2021 Evaluation of immune function in two populations of green sea turtles (*Chelonia mydas*) in a degraded versus a nondegraded habitat. *J. Wildl. Dis.* **57**, 761–772. (doi:10.7589/JWD-D-20-00204)
43. Blackburn NB *et al*. 2021 Transcriptomic profiling of fibropapillomatosis in green sea turtles (*Chelonia mydas*) From South Texas. *Front. Immunol.* **12**, 1–16. (doi:10.3389/fimmu.2021.630988)
44. Yetsko K *et al*. 2021 Molecular characterization of a marine turtle tumor epizootic, profiling external, internal and postsurgical regrowth tumors. *Commun. Biol.* **4**, 1–16. (doi:10.1038/s42003-021-01656-7)
45. Kane RA, Christodoulides N, Jensen IM, Becker DJ, Mansfield KL, Savage AE. 2021 Gene expression changes with tumor disease and leech parasitism in the juvenile green sea turtle skin transcriptome. *Gene* **800**, 145800. (doi:10.1016/j.gene.2021.145800)
46. Duffy DJ *et al*. 2018 Sea turtle fibropapilloma tumors share genomic drivers and therapeutic vulnerabilities with human cancers. *Commun. Biol.* **1**, 63. (doi:10.1038/s42003-018-0059-x)
47. Miller HC, Belov K, Daugherty CH. 2005 Characterization of MHC class II genes from an ancient reptile lineage, Sphenodon (tuatara). *Immunogenetics* **57**, 883–891. (doi:10.1007/s00251-005-0055-4)
48. Glaberman S, Caccone A. 2008 Species-specific evolution of class I MHC genes in iguanas (order: Squamata; subfamily: Iguaninae). *Immunogenetics* **60**, 371–382. (doi:10.1007/s00251-008-0298-y)
49. Jaratlerdsiri W, Isberg SR, Higgins DP, Gongora J. 2012 MHC class I of saltwater crocodiles (*Crocodylus porosus*): polymorphism and balancing selection. *Immunogenetics* **64**, 825–838. (doi:10.1007/s00251-012-0637-x)
50. McCafferty SS, Shorette A, Simundza J, Brennessel B. 2013 Paucity of genetic variation at an MHC Class I gene in Massachusetts populations of the diamond-backed terrapin (*Malaclemys terrapin*): a cause for concern? *J. Herpetol.* **47**, 222–226. (doi:10.1670/11-069)
51. Elbers JP, Taylor SS. 2016 Major histocompatibility complex polymorphism in reptile conservation. *Herpetol. Conserv. Biol.* **11**, 1–12.
52. Stiebens V, Merino SE, Chain FJJ, Eizaguirre C. 2013 Evolution of MHC class I genes in the endangered loggerhead sea turtle (*Caretta caretta*) revealed by 454 amplicon sequencing. *BMC Evol. Biol.* **13**, 1–11. (doi:10.1186/1471-2148-13-95)
53. Elbers JP, Clostio RW, Taylor SS. 2017 Neutral genetic processes influence MHC evolution in threatened gopher tortoises (*Gopherus polyphemus*). *J. Hered.* **108**, 515–523. (doi:10.1093/jhered/esx034)
54. Elbers JP, Brown MB, Taylor SS. 2018 Identifying genome-wide immune gene variation underlying infectious disease in wildlife populations – a next generation sequencing approach in the gopher tortoise. *BMC Genomics* **19**, 64. (doi:10.1186/s12864-018-4452-0)
55. Ehrhart LM, Redfoot WE, Bagley DA. 2007 Marine turtles of the central region of the Indian River Lagoon system. *Florida Sci.* **70**, 415–434.
56. Redfoot W, Ehrhart L. 2013 Trends in size class distribution, recaptures, and abundance of juvenile green turtles (*Chelonia mydas*) utilizing a rock riprap lined embayment at Port Canaveral, Florida, USA, as Developmental Habitat. *Chelonian Conserv. Biol.* **12**, 252–261. (doi:10.2744/ccb-0952.1)
57. Balazs GH. 1991 Current status of fibropapillomas in the Hawaiian green turtle, *Chelonia mydas*. In *Research plan for marine turtle fibropapilloma* (eds GH Balazs, SG Pooley), pp. 47–57. Washington, DC: U.S. Dep. Commer., NOAA Tech. Memo. NMFS-SWFSC.
58. Zhang J, Kobert K, Flouri T, Stamatakis A. 2014 PEAR: a fast and accurate illumina paired-end read mergeR. *Bioinformatics* **30**, 614–620. (doi:10.1093/bioinformatics/btt593)
59. Sebastian A, Herdegen M, Migalska M, Radwan J. 2016 Amplisas: a web server for multilocus genotyping using next-generation amplicon sequencing data. *Mol. Ecol. Resour.* **16**, 498–510. (doi:10.1111/1755-0998.12453)
60. Kearse M *et al*. 2012 Geneious basic: an integrated and extendable desktop software platform for the organization and analysis of sequence data. *Bioinformatics* **28**, 1647–1649. (doi:10.1093/bioinformatics/bts199)
61. Paradis E. 2010 Pegas: an R package for population genetics with an integrated-modular approach. *Bioinformatics* **26**, 419–420. (doi:10.1093/bioinformatics/btp696)
62. Paradis E, Schliep K. 2019 Ape 5.0: an environment for modern phylogenetics and evolutionary analyses in R. *Bioinformatics* **35**, 526–528. (doi:10.1093/bioinformatics/bty633)
63. Sievers F *et al*. 2011 Fast, scalable generation of high-quality protein multiple sequence alignments using Clustal Omega. *Mol. Syst. Biol.* **7**, 539. (doi:10.1038/msb.2011.75)
64. Kumar S, Stecher G, Tamura K. 2016 MEGA7: molecular evolutionary genetics analysis version 7.0 for bigger datasets brief communication. *Mol. Biol. Evol.* **33**, 1870–1874. (doi:10.1093/molbev/msw054)

65. Lanfear R, Frandsen PB, Wright AM, Senfeld T, Calcott B. 2016 PartitionFinder 2: new methods for selecting partitioned models of evolution for molecular and morphological phylogenetic analyses. *Mol. Biol. Evol.* **34**, 772–773. (doi:10.1093/molbev/msw260)
66. Ronquist F *et al.* 2012 MrBayes 3.2: efficient Bayesian phylogenetic inference and model choice across a large model space. *Softw. Syst. Evol.* **61**, 539–542. (doi:10.1093/sysbio/sys029)
67. Rambaut A, Drummond AJ, Xie D, Baele G, Suchard MA. 2018 Posterior summarization in Bayesian phylogenetics using tracer 1.7. *Syst. Biol.* **67**, 901–904. (doi:10.1093/sysbio/syy032)
68. Stamatakis A. 2014 RAxML version 8: a tool for phylogenetic analysis and post-analysis of large phylogenies. *Bioinformatics* **30**, 1312–1313. (doi:10.1093/bioinformatics/btu033)
69. Yu G, Smith DK, Zhu H, Guan Y, Lam TTY. 2017 ggtree: an R package for visualization and annotation of phylogenetic trees with their covariates and other associated data. *Methods Ecol. Evol.* **8**, 28–36. (doi:10.1111/2041-210X.12628.)
70. Leigh JW, Bryant D. 2015 POPART: full-feature software for haplotype network construction. *Methods Ecol. Evol.* **6**, 1110–1116. (doi:10.1111/2041-210X.12410)
71. Sidney J, Peters B, Frahm N, Brander C, Sette A. 2008 HLA class I supertypes: a revised and updated classification. *BMC Immunol.* **9**, 1–15. (doi:10.1186/1471-2172-9-1)
72. Sidney J, Grey HM, Kubo RT, Sette A. 1996 Practical, biochemical and evolutionary implications of the discovery of HLA class I supermotifs. *Immunol. Today* **17**, 261–266. (doi:10.1016/0167-5699(96)80542-1)
73. Sandberg M, Eriksson L, Jonsson J, Sjöström M, Wold S. 1998 New chemical descriptors relevant for the design of biologically active peptides. A multivariate characterization of 87 amino acids. *J. Med. Chem.* **41**, 2481–2491. (doi:10.1021/jm9700575)
74. Jombart T. 2008 adegenet: a R package for the multivariate analysis of genetic markers. *Bioinformatics* **24**, 1403–1405.
75. Brieuc MSO, Waters CD, Drinan DP, Naish KA. 2018 A practical introduction to Random Forest for genetic association studies in ecology and evolution. *Mol. Ecol. Resour.* **18**, 755–766. (doi:10.1111/1755-0998.12773)
76. Liaw A, Wiener M. 2002 Classification and regression in randomForest. *R News* **2**, 18–22.
77. Kuhn M. 2008 Building Predictive Models in R Using the caret Package. *J. Stat. Softw.* **28**, 1–26.
78. Lemeshow S, Hosmer DW, Klar J. 1988 Sample size requirements for studies estimating odds ratios or relative risks. *Stat. Med.* **7**, 759–764. (doi:10.1002/sim.4780070705)
79. Stevenson M *et al.* 2013 *Epir: an R package for the analysis of epidemiological data. R package version 0.9-48*. Vienna, Austria: R Foundation for Statistical Computing.
80. Ruxton GD, Neuhäuser M. 2013 Review of alternative approaches to calculation of a confidence interval for the odds ratio of a 2×2 contingency table. *Methods Ecol. Evol.* **4**, 9–13. (doi:10.1111/j.2041-210x.2012.00250.x)
81. Haldane JBS. 1940 The mean and variance of the moments of chi-squared when used as a test of homogeneity, when expectations are small. *Biometrika* **29**, 133–134.
82. Dunn OJ. 1961 Multiple comparisons among means. *J. Am. Stat. Assoc.* **56**, 52. (doi:10.2307/2282330)
83. Kosakovsky Pond SL, Posada D, Gravenor MB, Woelk CH, Frost SDW. 2006 Automated phylogenetic detection of recombination using a genetic algorithm. *Mol. Biol. Evol.* **23**, 1891–1901. (doi:10.1093/molbev/msl051)
84. Kosakovsky Pond SL, Frost SDW. 2005 Datamonkey: rapid detection of selective pressure on individual sites of codon alignments. *Bioinformatics* **21**, 2531–2533. (doi:10.1093/bioinformatics/bti320)
85. Kosakovsky Pond SL, Frost SDW. 2005 Not so different after all: a comparison of methods for detecting amino acid sites under selection. *Mol. Biol. Evol.* **22**, 1208–1222. (doi:10.1093/molbev/msi105)
86. Murrell B, Moola S, Mabona A, Weighill T, Sheward D, Kosakovsky Pond SL, Scheffler K. 2013 FUBAR: a Fast, Unconstrained Bayesian AppRoximation for inferring selection. *Mol. Biol. Evol.* **30**, 1196–1205. (doi:10.1093/molbev/mst030)
87. Murrell B, Wertheim JO, Moola S, Weighill T, Scheffler K, Kosakovsky Pond SL. 2012 Detecting individual sites subject to episodic diversifying selection. *PLoS Genet.* **8**, e1002764. (doi:10.1371/journal.pgen.1002764)
88. Stiebens VA, Merino SE, Roder C, Chain FJJ, Lee PLM, Eizaguirre C. 2013 Living on the edge: how philopatry maintains adaptive potential. *Proc. R. Soc. B* **280**, 20130305. (doi:10.1098/rspb.2013.0305)
89. Talarico L, Babik W, Marta S, Mattoccia M. 2019 Genetic drift shaped MHC IIB diversity of an endangered anuran species within the Italian glacial refugium. *J. Zool.* **307**, 61–70. (doi:10.1111/jzo.12617)
90. Eimes JA, Bollmer JL, Whittingham LA, Johnson JA, Van Oosterhout C, Dunn PO. 2011 Rapid loss of MHC class II variation in a bottlenecked population is explained by drift and loss of copy number variation. *J. Evol. Biol.* **24**, 1847–1856. (doi:10.1111/j.1420-9101.2011.02311.x)
91. Conant TA *et al*. 2009 Loggerhead sea turtle (*Caretta caretta*) 2009 status review under the U.S. Endangered Species Act. Report of the Loggerhead Biological Review Team to the National Marine Fisheries Service, August 2009.
92. Ene A, Su M, Lemaire S, Rose C, Schaff S, Moretti R, Lenz J, Herbst LH. 2005 Distribution of chelonid fibropapillomatosis-associated herpesvirus variants in Florida: molecular genetic evidence for infection of turtles following recruitment to neritic developmental habitats. *J. Wildl. Dis.* **41**, 489–497. (doi:10.7589/0090-3558-41.3.489)
93. Banerjee SM *et al.* 2021 Species and population specific gene expression in blood transcriptomes of marine turtles. *BMC Genomics* **22**, 1–16. (doi:10.1186/s12864-021-07656-5)
94. Jaeger CP, Duvall MR, Swanson BJ, Phillips CA, Dreslik MJ, Baker SJ, King RB. 2016 Microsatellite and major histocompatibility complex variation in an endangered rattlesnake, the Eastern Massasauga (*Sistrurus catenatus*). *Ecol. Evol.* **6**, 3991–4003. (doi:10.1002/ece3.2159)
95. Biedrzycka A *et al.* 2017 Extreme MHC class I diversity in the sedge warbler (*Acrocephalus schoenobaenus*); selection patterns and allelic divergence suggest that different genes have different functions. *BMC Evol. Biol.* **17**, 1–12. (doi:10.1186/s12862-017-0997-9)
96. Olivieri DN, Mirete-Bachiller S, Gambón-Deza F. 2020 MHC class I and II genes in Serpentes. *bioRxiv*, 1–12. (doi:10.1101/2020.06.12.133363)
97. Hedrick PW. 1999 Balancing selection and MHC. *Genetica* **104**, 207–214. (doi:10.1023/A:1026494212540)
98. Spurgin LG, Richardson DS. 2010 How pathogens drive genetic diversity: MHC, mechanisms and misunderstandings. *Proc. R. Soc. B* **277**, 979–988. (doi:10.1098/rspb.2009.2084)
99. Hughes AL, Ota T, Nei M. 1990 Positive Darwinian selection promotes charge profile diversity in the antigen-binding cleft of class I major-histocompatibility-complex molecules. *Mol. Biol. Evol.* **7**, 515–524. (doi:10.1093/oxfordjournals.molbev.a040626)
100. Savage AE, Zamudio KR. 2016 Adaptive tolerance to a pathogenic fungus drives major histocompatibility complex evolution in natural amphibian populations. *Proc. Biol. Sci.* **283**, 20153115. (doi:10.1098/rspb.2015.3115)
101. Jarvi SI, Tarr CL, Mcintosh CE, Atkinson CT, Fleischer RC. 2004 Natural selection of the major histocompatibility complex (Mhc) in Hawaiian honeycreepers (Drepanidinae). *Mol. Ecol.* **13**, 2157–2168. (doi:10.1111/j.1365-294X.2004.02228.x)
102. Madsen T, Ujvari B. 2006 MHC class I variation associates with parasite resistance and longevity in tropical pythons. *J. Evol. Biol.* **19**, 1973–1978. (doi:10.1111/j.1420-9101.2006.01158.x)
103. Nowak MA, Tarczy-Hornoch K, Austyn JM. 1992 The optimal number of major histocompatibility complex molecules in an individual. *Proc. Natl Acad. Sci. USA* **89**, 10 896–10 899. (doi:10.1073/pnas.89.22.10896)
104. Wegner KM, Kalbe M, Kurtz J, Reusch TBH, Milinski M. 2003 Parasite selection for immunogenetic optimality. *Science* **301**, 1343. (doi:10.1126/science.1088293)
105. Lenz TL, Becker S. 2008 Simple approach to reduce PCR artefact formation leads to reliable genotyping of MHC and other highly polymorphic loci—implications for evolutionary analysis. *Gene* **427**, 117–123. (doi:10.1016/j.gene.2008.09.013)
106. Rekdal SL, Anmarkrud JA, Johnsen A, Lifjeld JT. 2018 Genotyping strategy matters when analyzing hypervariable major histocompatibility complex—experience from a passerine bird. *Ecol. Evol.* **8**, 1680–1692. (doi:10.1002/ece3.3757)
107. Reusche MR. 2020 *Genetic structure of green sea turtle (Chelonia mydas) foraging aggregations on the east coast of Florida*. Orlando, FL, USA: University of Central Florida. See https://stars.library.ucf.edu/honorstheses/750.

108. Shamblin BM *et al.* 2014 Geographic patterns of genetic variation in a broadly distributed marine vertebrate: new insights into loggerhead turtle stock structure from expanded mitochondrial DNA sequences. *PLoS ONE* **9**, e85956. (doi:10.1371/journal.pone.0085956)
109. Cutrera AP, Lacey EA. 2007 Trans-species polymorphism and evidence of selection on class II MHC loci in tuco-tucos (Rodentia: Ctenomyidae). *Immunogenetics* **59**, 937–948. (doi:10.1007/s00251-007-0261-3)
110. Minias P, Bateson ZW, Whittingham LA, Johnson JA, Oyler-Mccance S, Dunn PO. 2016 Contrasting evolutionary histories of MHC class I and class II loci in grouse—effects of selection and gene conversion. *Heredity (Edinb.)* **116**, 466–476. (doi:10.1038/hdy.2016.6)
111. Go Y, Satta Y, Kawamoto Y, Rakotoarisoa G, Randrianjafy A, Koyama N, Hirai H. 2002 Mhc-DRB genes evolution in lemurs. *Immunogenetics* **54**, 403–417. (doi:10.1007/s00251-002-0480-6)
112. Klein J. 1987 Origin of major histocompatibility complex polymorphism: the trans-species hypothesis. *Hum. Immunol.* **19**, 155–162. (doi:10.1016/0198-8859(87)90066-8)
113. Těšický M, Vinkler M. 2015 Trans-species polymorphism in immune genes: general pattern or MHC-restricted phenomenon? *J. Immunol. Res.* **2015**, 838035. (doi:10.1155/2015/838035)
114. Klein J, Sato A, Nagl S, O'hUigín C. 1998 Molecular trans-species polymorphism. *Annu. Rev. Ecol. Syst.* **29**, 1–21.
115. Dudek K, Gaczorek TS, Zieliński P, Babik W. 2019 Massive introgression of major histocompatibility comple2x (MHC) genes in newt hybrid zones. *Mol. Ecol.* **28**, 4798–4810. (doi:10.1111/mec.15254)
116. Sagonas K, Runemark A, Antoniou A, Lymberakis P, Pafilis P, Valakos ED, Poulakakis N, Hansson B. 2019 Selection, drift, and introgression shape MHC polymorphism in lizards. *Heredity (Edinb.)* **122**, 468–484. (doi:10.1038/s41437-018-0146-2)
117. Naro-Maciel E, Le M, FitzSimmons NN, Amato G. 2008 Evolutionary relationships of marine turtles: a molecular phylogeny based on nuclear and mitochondrial genes. *Mol. Phylogenet. Evol.* **49**, 659–662. (doi:10.1016/j.ympev.2008.08.004)
118. Karl SA, Bowen BW, Avise JC. 1995 Hybridization among the ancient mariners: characterization of marine turtle hybrids with molecular genetic assays. *J. Hered.* **86**, 262–268. (doi:10.1142/9789814317764_0004)
119. Soares LS *et al.* 2018 Effects of hybridization on sea turtle fitness. *Conserv. Genet.* **19**, 1311–1322. (doi:10.1007/s10592-018-1101-8)
120. James MC, Martin K, Dutton PH. 2004 Hybridization between a green turtle, *Chelonia mydas*, and loggerhead turtle, *Caretta caretta*, and the first record of a green turtle in Atlantic Canada. *Can. Field-Naturalist* **118**, 579–582. (doi:10.22621/cfn.v118i4.59)
121. Shamblin BM, Mansfield KL, Seney EE, Long CA, Bagley DA, Nairn CJ. 2018 Brazilian origin of a neritic juvenile hybrid loggerhead×green turtle foraging in Florida. *Mar. Turt. Newsl.* **155**, 4–7.
122. Sandmeier FC, Tracy RC. 2014 The metabolic pace-of-life model: incorporating ectothermic organisms into the theory of vertebrate ecoimmunology. *Integr. Comp. Biol.* **54**, 387–395. (doi:10.1093/icb/icu021)
123. Zimmerman LM. 2018 Reptilia: humoral immunity in reptiles. In *Advances in comparative immunology* (ed. E Cooper), pp. 751–772. Cham, Switzerland: Springer.
124. Sandmeier FC, Tracy CR, DuPré S, Hunter K. 2012 A trade-off between natural and acquired antibody production in a reptile: implications for long-term resistance to disease. *Biol. Open* **1**, 1078–1082. (doi:10.1242/bio.20122527)
125. Long CA, Chabot RM, El-Khazen MN, Kelley JR, Mollet-Saint Benoît C, Mansfield KL. 2021 Incongruent long-term trends of a marine consumer and primary producers in a habitat affected by nutrient pollution. *Ecosphere* **12**, e03553. (doi:10.1002/ecs2.3553)
126. Keller JM, Balazs GH, Nilsen F, Rice M, Work TM, Jensen BA. 2014 Investigating the potential role of persistent organic pollutants in Hawaiian green sea turtle fibropapillomatosis. *Environ. Sci. Technol.* **48**, 7807–7816. (doi:10.1021/es5014054)
127. Congdon JD, Dunham AE, Van Loben Sels RC. 1993 Delayed sexual maturity and demographics of Blanding's turtles (*Emydoidea blandingii*): implications for conservation and management of long-lived organisms. *Conserv. Biol.* **7**, 826–833. (doi:10.1046/j.1523-1739.1993.740826.x)
128. Zimmerman LM, Vogel LA, Bowden RM. 2010 Understanding the vertebrate immune system: insights from the reptilian perspective. *J. Exp. Biol.* **213**, 661–671. (doi:10.1242/jeb.038315)
129. Martin, KR, Mansfield KL, Savage, AE. 2021 Data from: adaptive evolution of MHC class I immune genes and disease associations in coastal juvenile sea turtles. *Zenodo* (doi:10.5281/zenodo.5703775)
130. Martin, KR, Mansfield KL, Savage, AE. 2022 Adaptive evolution of major histocompatibility complex class I immune genes and disease associations in coastal juvenile sea turtles. Figshare.